JOURNAL OF MATERIALS SCIENCE 27 (1992) 1271–1274

Laser processing of NiCrAlFe alloy: microstructural evolution

J. J. de DAMBORENEA, A. J. VÁZQUEZ
Centro Nacional de Investigaciones Metalúrgicas Avenida de Gregorio del Amo, 8 E-28040 Madrid, Spain

Laser surface treatments are an attractive alternative for the production of new materials with high mechanical and corrosion-resistance properties. This technique permits the production of materials with a high added value on low-cost materials. The present research is aimed at obtaining NiCrAl alloys on iron-based materials using a continuous CO_2 laser with 5–7 kW power. The microstructural characteristics and influence of iron on the type of phase in the new alloy is also analysed.

1. Introduction

The incessant demand for technologically advanced materials which can work at extreme temperatures and pressure have led to the development of new products that can satisfy the needs of industry. In the field of metals, alloys based on so-called super-alloys are being pursued. In simple terms, superalloys are especially [1] (a) rich in at least nickel, cobalt, titanium, niobium and/or iron, and (b) able to maintain their structural properties as well as surface stability and properties in severe environments under high temperatures and pressure. Other properties such as low density and cost are also required [2].

The mechanism used to resist oxidation at high temperatures by MCrAl alloys, in which M may be one of the above-mentioned predominant elements, is primarily due to the combination of the properties of each alloying agent, particularly the aluminium content. Aluminium is responsible for the formation of Al_2O_3-rich scales aimed at avoiding the diffusion of elements and acting as a barrier layer and, then, conferring protection from degradation by oxidation and high-temperature corrosion. Rare-earths of the Hf or Y type are sometimes added because they improve the adherence of the oxide layers during thermal cycling.

The search for materials which can resist this new situation has meant that complex alloys with up to ten elements have been formulated. Because the elements forming part of these materials are scarce, and industrialized countries are almost totally dependent on Third World countries for the elements in the superalloys, alternative production methods are being studied to save material. Surface engineering has arisen in this environment, and involves the production of new materials using techniques of surface modification. Laser is one of the most attractive techniques because of its versatility and the possibility of obtaining high-value surface alloys on low-cost materials.

The present research project studied the production of NiCrAl alloy on carbon steels from the perspective of their metallographic characteristics. The corrosion behaviour results will be presented in a future paper.

2. Experimental procedure

The particle injection technique was used for the surface alloying. This technique involves the injection of the correctly mixed alloy powder on to a laser beam with the appropriate power. When the powder intercepts the beam, it melts and is deposited on the surface of the base metal, thus providing a uniform layer of the injected alloy, which is diluted in accordance with the parameters of the process. The experimental design is thoroughly explained by Weerashinge *et al.* [3].

The powder we used included several chemically pure elements with an elemental powder particle size between 10 and 100 μm. The nominal composition of the initial alloy was (in atomic percentages): 60% Ni, 26.5% Cr and 13.5% Al.

Prior to alloying, the powders were mechanically stirred for 12 h and dried. The drying process was carried out by heating the powders in a furnace at 200 °C for about 12 h followed by slow cooling to room temperature. The powder feed rate was set by the design of the feeder, one of the type commonly used for plasma spraying, which only permits a minimum flow of 76 g min^{-1}. The powders used were subjected to parallel pneumatic shaking in the feeder. Nickel, chrome and aluminium powders were chosen because of their corrosion resistance properties at high temperatures.

The laser we used was an industrial ML-108 generator from LASER MELIS, a FAGOR CO_2 continuous wave and a high-frequency electrical discharge, able to supply a variable power beam of up to 8 kW operating in the range of 5–7 kW. The beam leaves the generator in the form of a uniformly illuminated ring and is guided by a system of mirrors to a beam integrator which transforms the ring into a 1 cm^2 rectangle. The relative beam/material movement is

0022–2461

achieved using a three axis table with numerical control. The processing speeds used were 1.7 and 6.7 mm s^{-1} according to the power used, either 5, 6 or 7 kW. The power level of the generator during the process was controlled by a closed cycle system which maintained it constant within a range of $\pm$ 2%, thus ensuring the uniformity of the thermal input [4].

Mild carbon steel was used as the base material for the preparation of the layers. Their composition was (wt %) C 0.46, Si 0.18, Mn 0.46, P 0.024, S 0.039, Cu 0.35, Cr 0.10, Ni 0.11, and its metallographical structure, of ferrite and pearlite, is shown in Fig. 1. The base steel was chosen for two reasons: (i) the production of high-performance material on an economical base, and (ii) to analyse the influence of the iron.

Alloying was carried out in an argon atmosphere to minimize surface oxidation of the resultant layers.

Once the alloys were obtained, they were studied by optical and scanning electron microscopy with EDS X-ray analysis. In all cases, compositional analysis (EDS) of a typical alloyed layer showed a reasonable degree of homogeneity. The metallographic observations were done on transverse cuts in the material which, after polishing, were attacked by a mixture of nitric and hydrochloric acid and alcohol, with either a Marble or Murakami rective.

3. Results and discussion

Of the three powers and two speeds, the best results were obtained at 7 kW and 1.67 mm s^{-1}, constituting a thermal input of 400 J mm^{-2}. The macrograph in Fig. 2 shows a general view of a plating on carbon steel. This macrograph is representative of all the samples obtained. The plated layer has a depth of approximately 2 mm, while that of the molten substratum is 0.7 mm. The bead width is 11 mm, matching the diameter of the beam which produced it. According to calculations deduced from the figure, the dilution is 25% [5].

Fig. 3 shows detail of the interface. A large interfacial area can be seen which is divided into two parts. There was a double Nital-based attack on the steel base and a Murakami attack on the track, permitting

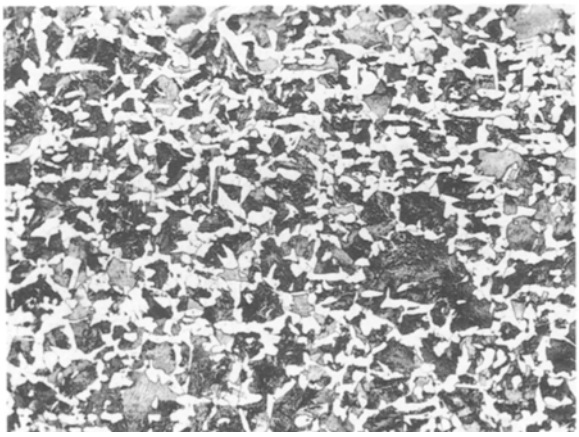

Figure 1 Metallographical structure of the mild steel. Etching with Nital 2%, × 200.

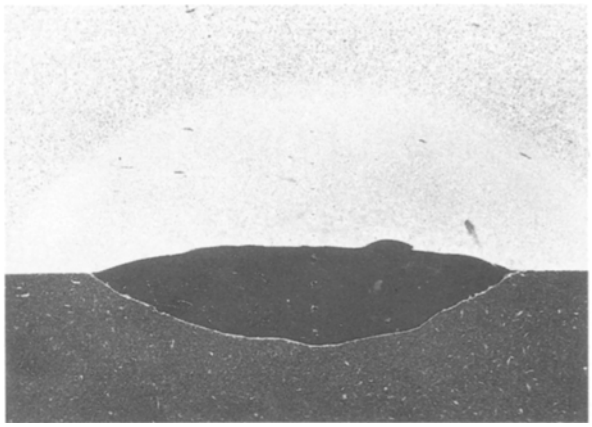

Figure 2 Optical macrograph of the laser track, × 7.

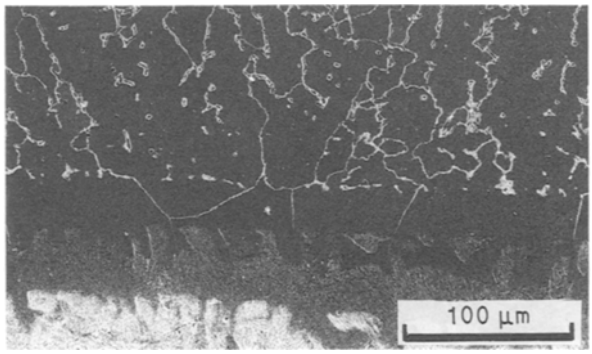

Figure 3 Interface between the alloyed zone and the track. Etching with Nital 2% for the base material and Murakami for the track.

two areas to be distinguished. The iron-rich internal interface, where a slight dilution of the alloy elements can be observed, is perfectly defined without any type of crack or unevenness. There is no specific structure in the interface closest to the track, although clearly defined grains can be discerned. The X-ray microanalysis performed on both sides of the interface revealed the compositions shown in Table I.

Moving from the interface towards the internal surface of the track, a base with dendritic grain boundaries in which there is a clear second phase, can be seen Fig. 4. Fig. 4b also clearly shows small spherical dots which are evenly distributed throughout the alloy layer.

The micrograph in Fig. 5, of a sample without metallographic attack, shows a secondary image of both structures. Their phase shape and distribution is similar until the final part of the coating.

A detailed analysis of the different metallographic structures in the plating obtained from the energy dispersion technique is set out in Table II. In the table, the spherical and second phase, spread uniformly throughout the sample and on the edge, respectively, can be clearly distinguished. The spherical forms have a rich aluminium content and are low in the other elements, except for oxygen, obtained from the difference. The structures on the grain boundary are richer in aluminium than the base, reaching up to 25 at %. Finally, the central and external parts of the whole material were analysed at 500 and 1000 μm from the

TABLE I Compositions revealed by X-ray analysis

Internal interphase (steel side, at %)	1.1 Al, 85.7 Fe, 8.45 Ni, 4.1 Cr, 0.65 others
External interphase (track side, at %)	6.6 Al, 48.6 Fe, 31.5 Ni, 12.9 Cr, 0.4 others

TABLE II Analysis of metallographic structures

	Composition (at %)				
	Ni	Cr	Al	Fe	O
Spherical particles	1.8	1.2	51.8	1.4	43.8
Second phase	50	11	25	14	–

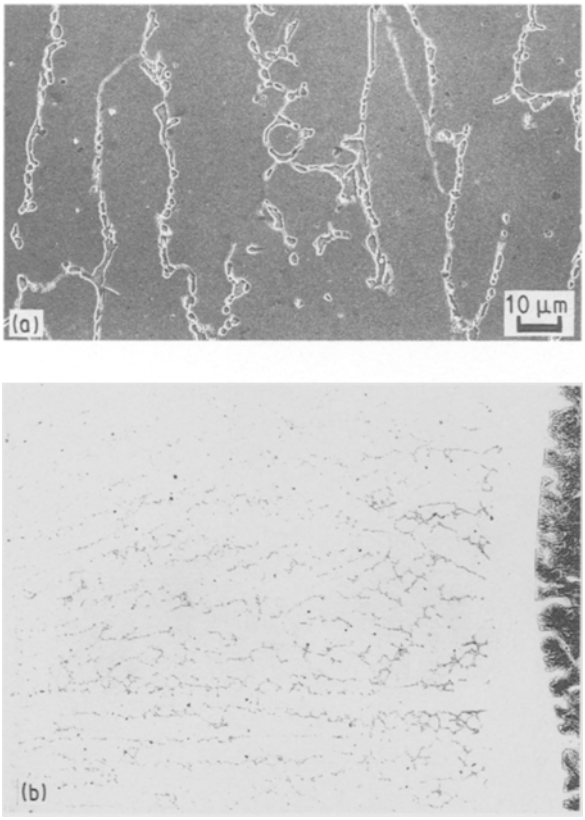

Figure 4 (a) Second phase in the dendritic grain boundaries. (b) Small spherical dots distributed throughout the track. Etching with hydrochloric and nitric acids and alcohol.

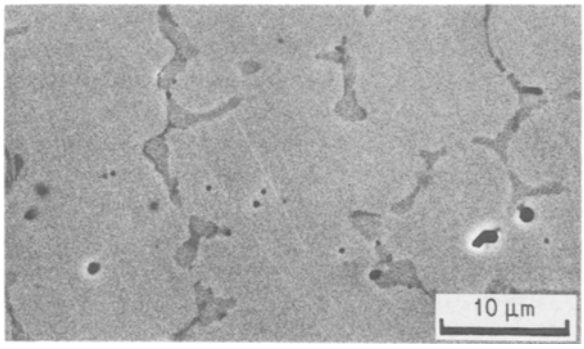

Figure 5 Secondary image of the structures without attack.

interface. The compositions (at %) were similar in both areas: Al 11.0, Fe 25.0, Ni 45.0, Cr 19.0. These were quite similar to the composition of the initial powder, although the final composition was affected by the presence of iron as a result of the degree of dilution, with the proportion of the alloy agents remaining practically constant and relatively close to that found from the initial calculation.

A first approach to the structures found in the first phase ought to be based on the balance diagrams. According to the pioneering work by Taylor and Floyd [6], it is possible to predict the phases for a given initial composition. Nevertheless, the information is only partially valid because of the temperatures reached during the process, the entrance of a fourth element, such as iron, and the high solidification speed on leaving the system, are far from a phase equilibrium state. Taking the 1250 and 1200 °C isotherm found by Merchant and Notis [7] as a reference point, the base alloy is situated in the γ phase field of stability. However, analyses of the compositions obtained indicate the presence of other phases. These compositions prove the presence of aluminium oxide in the form of Al_2O_3, which is finely spread throughout the alloy, γ', Ni_3Al, defined by the 25 at % Al, and a solid solution of iron, chromium and aluminium in nickel which, according to these analyses, can be identified as γ phase.

With an alloy of 54 Ni, 30 Cr, 11 Al and 3.75 Fe (at %), Jasmin and West [8] have found that the solidification sequence in the iron-rich regions near the substratum can be described as a γ phase followed by a eutectic transformation of $\beta + \gamma$ in the initial phase. The central region of the track is predominantly $\beta + \gamma$, with a γ' phase in the dendritic structure of the upper part. The results presented here are somewhat similar, although the metallographic structures and compositions do not vary greatly in the alloy layer except for the interfacial zone. The laser parameters (power, speed and feed) used in the experiment, as well as the higher iron content in the final composition, may be the cause of the difference.

The appearance of aluminium oxide may be due to the high reactivity of the aluminium powder used. Thus the powder oxidized and was incorporated into the base in an oxide form during the surface alloying process. The subsequent effects on the properties of the alloy are currently being analysed.

Special attention should also be given to appearance of the γ' phase and its relationship to the iron which appears in the coating as a result of the dilution. According to Singh and Mazumder [9], when it is in more than 10 at % concentration, iron tends to replace the nickel, forming an $(Ni, Cr, Fe)_3Al$ intermetallic compound. This property could modify the mechanical and high-temperature resistance behaviour of the alloy in a positive manner. Furthermore, the presence of iron could act as a motor for the precipitation of γ' which under normal conditions is only achieved after prolonged thermal treatment or by alloying with other rare-earth elements such as Hf or Y.

Acknowledgement

The authors wish to thank the Interministerial Commission for Science and Technology (CICYT) for funding the project MAT88-0144 which was responsible for financing this study.

References

1. W. BOESCH, in "Superalloys, supercomposites and superceramics", edited by J. Tien and T. Caulfield (Academic Press, San Diego, 1989) pp. 1–7.
2. J. L. GONZÁLEZ, P. ADEVA and M. ABALLE, *Rev. Metal. Madrid* **25**(3) (1989) 195.
3. V. M. WEERASHINGE, W. M. STEEN and D. R. F. WEST, *Surface Engng* **3** (1987) 147.
4. J. de DAMBORENEA, M. DORRONSORO, A. J. VÁZQUEZ and V. LÓPEZ, in "Laser 5, Laser Materials Processing for Industry", edited by S. Gosh (IITT, Paris, 1989) pp. 173–8.
5. G. J. BRUCK, *J. Metals* **39** February (1987) 10.
6. A. T. TAYLOR and R. W. FLOYD, *J. Inst. Metals* **81** (1952–1953) 451.
7. S. M. MERCHANT and M. R. NOTIS, *Mater. Sci. Engng* **66** (1984) 47.
8. K. M. JASIM and D. R. F. WEST, in "Proceedings of the Materials Research Society Symposium" Vol. 129 (MRS, Pittsburg, 1989) pp. 139–44.
9. J. SINGH and J. MAZUMDER, in "Proceedings of the 3rd International Conference on Lasers in Manufacturing" edited by A. Quenzer (IFS, Bedford, 1986) pp. 169–79.

Received 3 December 1990
and accepted 10 April 1991